Experiments in Fluids 37 (2004) 645–652
DOI 10.1007/s00348-004-0846-7

Structure and dynamics of a bidimensional pattern of liquid columns

P. Brunet, G. Gauthier, L. Limat, D. Vallet

Abstract We report an experimental study of the structure and dynamics of a bidimensional array of liquid columns. This pattern is formed below a flat porous plate continuously supplied with liquid. It exhibits a marked hexagonal tendency. Its typical wavelength is close to that of the most dangerous mode of the Rayleigh–Taylor instability of a thin viscous layer hanging below a plate, defined by the competition between gravity and surface tension. Collective dynamical behaviors are also evidenced, involving oscillations of the column positions, columns migrations, coalescences and nucleations. Quantitative comparisons are presented with the equivalent one-dimensional pattern formed below the perimeter of an overflowing dish ("circular fountain experiment").

1 Introduction

A viscous layer hanging below a horizontal substrate is known to undergo instability, leading to the formation of networks of pendent drops (Hynes 1978; Yiantsios and Higgins 1989; Fermigier et al. 1992). This instability is a particular case of the famous Rayleigh–Taylor instability, investigated long ago by Rayleigh (1900) and Taylor (1950), except that viscosity, instead of inertia, governs kinetics here. This cross-over between inertia-dominated situations and viscosity-dominated situations has motivated several works (Chandrasekhar 1961; Plesset and Whipple 1974), a classification of the possible regimes being available in Limat (1993). Among the results discussed in this reference, it turns out that provided that the layer is thin enough compared to the capillary length $l_c = \frac{\gamma}{\rho g}$ (γ surface tension, ρ liquid density, g acceleration of gravity) and to a viscous scale $l_v = (\frac{\eta^2}{\rho^2 g})^{1/3}$, the final lattice of the pendant drop exhibits a typical wavelength:

$$\lambda_M = 2\pi\sqrt{2}l_c. \quad (1)$$

This is in very good agreement with both experiments (Fermigier et al. 1992) and numerical simulations (Yiantsios and Higgins 1989). A typical picture of the experiments reported in Fermigier et al. (1992) is reproduced in Fig. 1a. This experiment also reveals a marked tendency of this system to favor the hexagonal symmetry, a fact also mentioned long ago by Whitehead et al. for experiments carried out with moderately thick layers of viscous fluids (1975).

The Rayleigh–Taylor (RT) instability of a thin layer occurs in many natural or applied situations (geophysics, technical devices involving films, bubble emission in film boiling, etc.). On the other hand, in many of these applications, the unstable layer is an open system exchanging liquid with an external source. One can think of, among other examples, film-boiling experiments (Berenson 1962), diapir formation in geophysics (Whitehead et al. 1975), or film flows in tubular heat exchangers (Ganic and Roppo 1980). In these devices, a liquid cascades onto a series of horizontal tube, with RT instability occurring below each tube. A natural question here is how this external supply of liquid modifies the typical features of the obtained pattern. This question has been investigated in 1-D in two experiments (Giorgiutti et al. 1995; Counillon et al. 1998; Brunet 2002; Brunet et al. 2001), below a single horizontal tube and below the perimeter of a circular overflowing fountain respectively (see Fig. 1b and c). At a low flow rate, RT instability combined with the external supply leads to the appearance of a regular network of pendent drops, from which smaller falling drops are emitted at a well-defined frequency. At a higher flow rate this pattern is replaced by a remarkably regular pattern of liquid columns whose wavelength is a bit smaller than that expected from Eq. 1.

This result was not in fact so new, as observations of the dripping and column regimes are available in the technical literature relative to tubular heat exchangers (Ganic and Roppo 1980), or in previous investigations of similar flows performed in a different context (Carlomagno 1974; Pritchard 1986). On the other hand, a remarkable fact reported in (Giorgiutti et al. 1995; Counillon et al. 1998; Brunet et al. 2001) was that the array of liquid columns exhibits complex spatio–temporal behaviors suggested in Fig. 2. Depending on the possible symmetry-breaking of the interface connecting two columns, these ones can remain

Received: 02 December 2003 / Accepted: 20 June 2004
Published online: 19 August 2004

P. Brunet (✉), G. Gauthier, L. Limat, D. Vallet
Laboratoire de Physique et Mécanique des Milieux Hétérogènes
UMR7636 CNRS, Ecole Supérieure de Physique et Chimie Industrielles, 10, rue Vauquelin, 75231
Paris Cedex 05, France
E-mail: brunet@mech.kth.se

L. Limat
Fédération de Recherche Matière et Systèmes Complexes,
FR 2438 CNRS, France

Present address: P. Brunet
Department of Mechanics, Kungliga Tekniska Hogskolan,
10044, Stockholm, Sweden

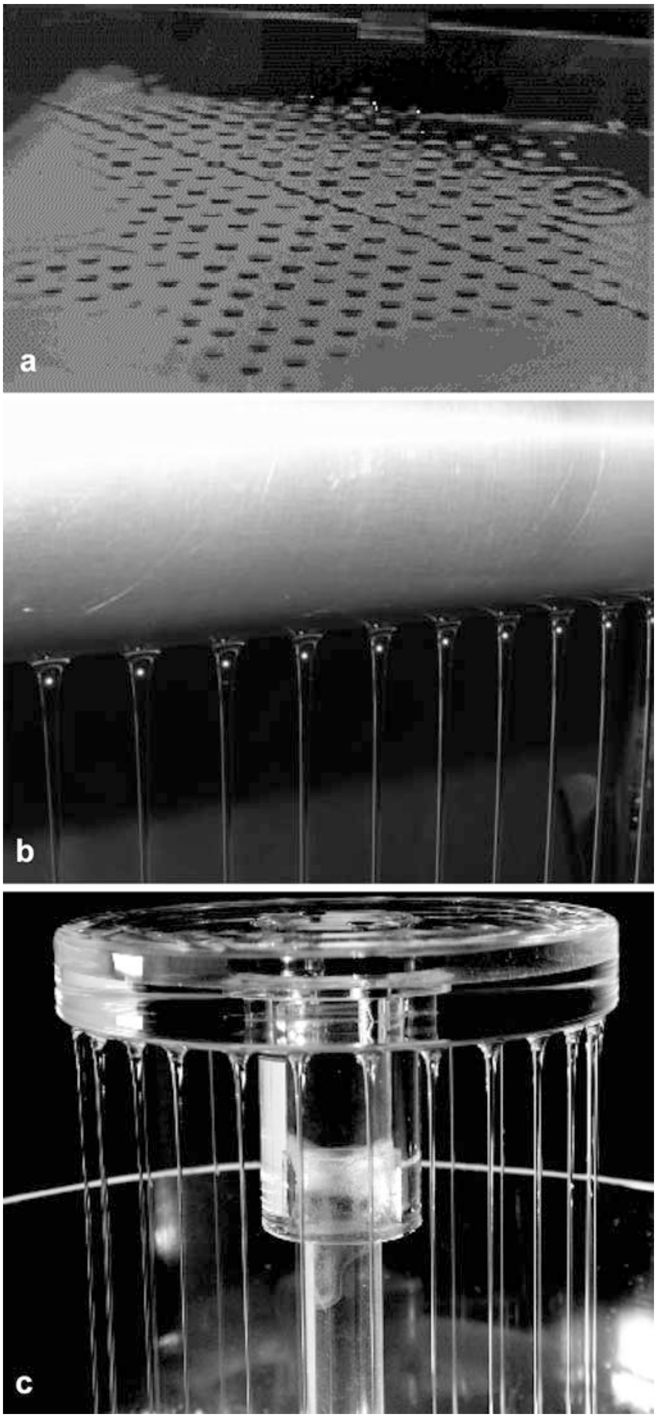

Fig. 1a–c. Experiments connected to those presented in this article. **a** Network of pending drops under a plate (from Fermigier et al. 1992). **b** Array of liquid columns under an overflowing hollow cylinder. **c** Array of liquid columns under an overflowing circular dish

static (Fig. 2a), or can undergo a drift at a constant speed (Fig. 2b) or oscillations of the column positions (Fig. 2c). Non-trivial combinations of these two last states, with coalescences/nucleations phenomena, can lead to increasing complexity with the possible appearance of spatio–temporal chaos (Brunet 2002; Brunet et al. 2001). These behaviors are very similar to those observed in other one-dimensional pattern forming instabilities (Flesselles et al. 1991; Cross and Hohenberg 1993) that have raised considerable interest in non-linear physics.

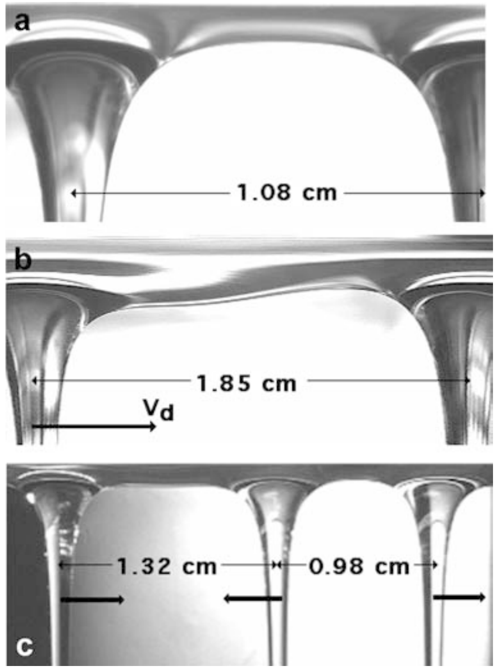

Fig. 2a–c. Typical possible states of a cell inside a 1-D pattern of liquid columns. The motion is indicated by *arrows*. **a** Symmetrical arch connecting two static columns. **b** Asymmetrical, dilated arch between two drifting columns. **c** Symmetrical, alternatively dilated or shrunk arches between oscillating columns

A question now still open is what would happen when this modified Rayleigh–Taylor instability under continuous supply is combined with a 2-D geometry similar to that of Fig. 1a. Will the hexagonal symmetry reported in Fermigier et al. (1992) be observed again? How will the dynamics be affected? To investigate these questions we have devised a simple experiment in which columns are formed below a horizontal porous plate continuously fed with liquid (Brunet 2002). This experiment is described in the present paper together with the first results recently obtained. As we shall see, spectacular 2-D networks of liquid columns are observed, with the expected tendency to form hexagonal structures. The observed wavelengths are compared to their equivalents in 1-D. As we shall see the wavelengths dependence upon flow-rate are very similar in 1-D and 2-D, the values remaining close to that from in Eq. 1. The dependence of the oscillations frequency versus flow-rate is also very similar in 1-D and 2-D except that quantitative differences seem to be involved. Finally, qualitative differences are observed concerning the transition towards spatio–temporal chaos. In the 2-D case, there exist stable fronts bordering on disordered and static domains. This is not observed in 1-D, where disorder always spreads through the whole pattern.

A similar network of liquid columns has also been reported and investigated in another experiment published recently (Pirat et al. 2004), with rather different boundary conditions (column positions rigidly fixed at the boundaries). The same tendency to form a hexagonal network was also observed, together with dynamics phenomena specific to these conditions.

2
Experimental setup

The experimental setup is suggested in Fig. 3a. A liquid (silicon oil) put into motion by a gear pump (ISMATEC BVP-Z (a)), flows across a flow-meter (b), and is continuously supplied to a partially-filled cylindrical chamber (c). This chamber is made of a Plexiglas cylinder and two steel plates, a large hole 15 cm in diameter being drilled in the bottom. In this hole, a "porous medium" is inserted, constituted by a thick packing (thickness h = 10 mm) of mono-disperse spherical glass balls (diameter d = 1.5 mm) compressed between two parallel flat rigid steel grids (see Fig. 3b). The liquid flows across the porous medium, and accumulates below the lowest grid where it undergoes a Rayleigh–Taylor instability. At a high enough flow-rate, this instability leads to a 2-D pattern of liquid columns (d) reproduced in Fig. 3c).

The grid used is also visible in this figure. To limit as much as possible any bias introduced by the grid structure, we have used an "isotropic" grid of triangular symmetry (plates drilled with a triangular lattice of holes), whose typical mesh (1 mm) is small compared to the natural scale of the pattern (centimetric scale). We have not observed any particular change when trying to modify the grid mesh. The total surface of the grid, across which the liquid is flowing is a circular disk ϕ=15 cm in radius, surrounded by a metal rim, also visible in the figure. In order to avoid that too much liquid remains captured by the metal rim surrounding the grid, a very thin circular mask 7 cm in radius is placed between the grid and the packing of spheres. This preserves the circular boundary conditions imposed by the rim and avoids the observation of unphysical columns spots in the pictures taken from below. Later, hexagonal masks were also introduced (see next part) to change these boundary conditions and to improve the hexagonal tendencies observed for this pattern.

The horizontality of the chamber, i.e., of the lowest grid, is tuned by a three-screws system. Also, the liquid level inside the chamber is selected by opening and closing a hole drilled across the upper steel plate of the cell. Using this half-filled chamber allows us to damp the possible residual perturbations introduced by the pump. Also, by controlling the constancy of the liquid level, one can check that the system has reached a stationary state with a well-defined, constant and uniformly distributed flow rate across the grids. Note also that the presence of the porous medium is very helpful to limit the flow across the grids. In fact, in some sense, we are looking at a pattern formed on a liquid film hanging below a grid, the porous medium being here only to regularize and limit the flow. A different strategy, used by the Nice group (INLN) consists in using only a single grid without the porous medium and controlling the pressure inside the chamber. Playing with this pressure allows one also to control the level of liquid inside the chamber. In our opinion this difference should not matter too much for the pattern properties.

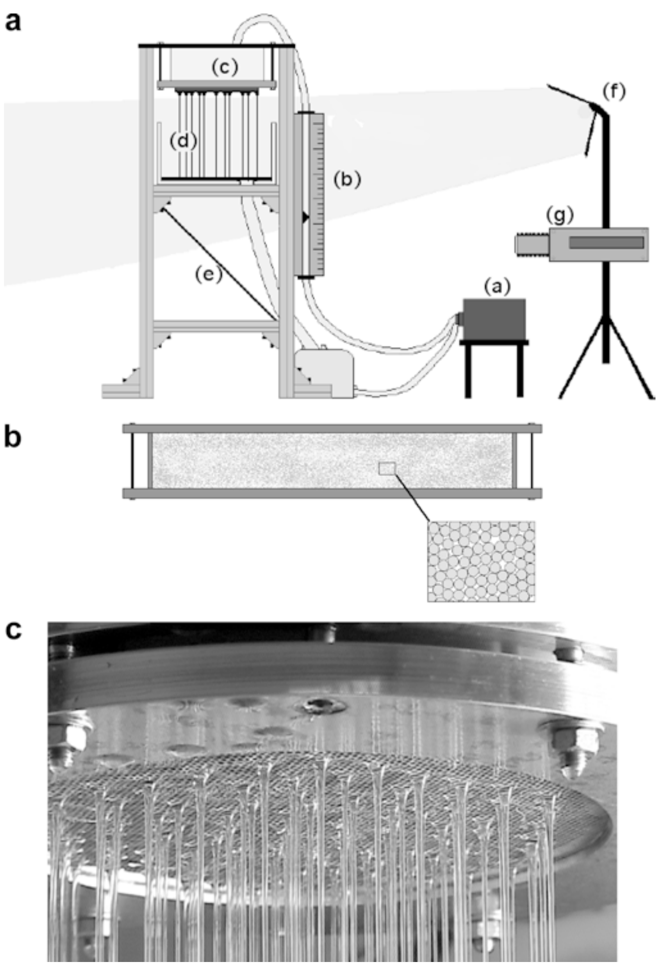

Fig. 3. a Sketch of the experimental setup. **b** Magnified view of the porous medium used, confined between two grids. **c** An example of the 2-D pattern of liquid columns formed below the lowest grid

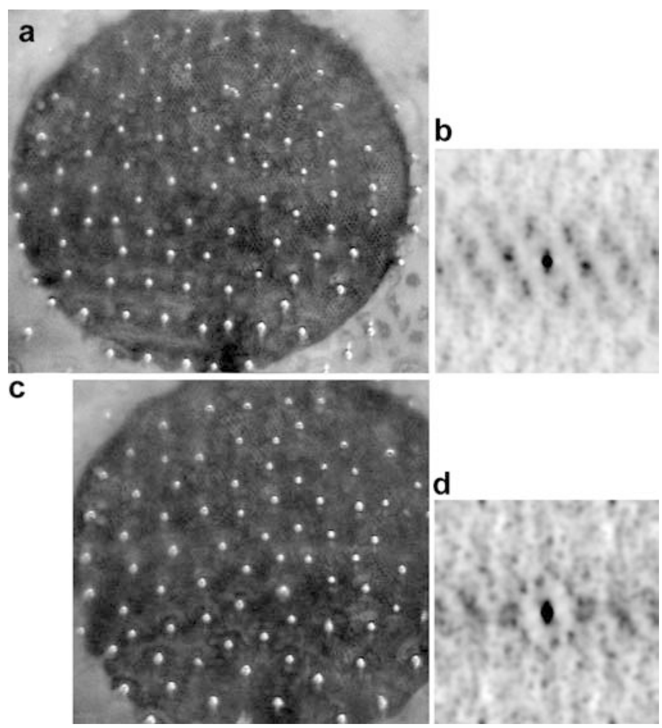

Fig. 4a–d. Bidimensional lattice of liquid columns viewed from below, η=50 cP and with circular boundaries. **a** Q=36.0 cm^3/s. **b** Autocorrelation of **a**. **c** Q=64.0 cm^3/s. **d** Autocorrelation of **c**

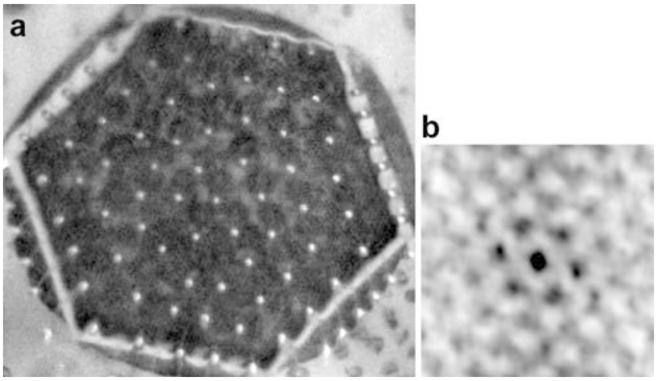

Fig. 5a, b. Bidimensional lattice of liquid columns viewed from below with hexagonal boundaries. **a** Q=29.7 cm^3/s, η=50 cP. **b** Autocorrelation of **a**

Concerning the liquid, we have used two silicon oils of viscosity equal to η=20 cP and η=50 cP respectively. The surface tension was equal to γ=20.6 dyn/cm, and γ=20.7 dyn/cm respectively, while the mass density was ρ=0.95 g/cm^3 and ρ=0.96 g/cm^3 respectively.

3
Qualitative description of the flow

We have reproduced in Fig. 4a and c two typical pictures of the pattern taken from below. Nearly 90 columns (with a typical variation of ±8 units) constitute the pattern. In these first experiments, the oil was flowing across the whole grid, circular boundary conditions being provided by the metal rim surrounding this grid. To be more precise, the thickness of this metal rim is such that the grid is in fact surrounded by a cylindrical vertical wall on which oil is flowing. At first sight, in these circular boundary conditions a certain tendency towards a hexagonal geometry is observed but with a very strong disorder. To check it, we have extracted from these figures spatial autocorrelation pictures reproduced in Fig. 4b and d. Just as the initial pictures, these diagrams are matrices of grey levels on which a point at coordinate (x, y) will be dark if the initial picture is spatially well-correlated to its image translated to the (x, y) vector. At least the first of these diagrams confirms the hexagonal tendency exhibited by this 2-D pattern of liquid columns. Let us also mention that with this circular boundary condition, the pattern is never static, with the irregular and endless motions of the columns being observed suggesting a state of permanent spatio–temporal chaos. Obviously, the presence of the circular boundary condition is incompatible with the observance of a regular hexagonal network.

In a second set of experiments, we have tried to amplify the hexagonal tendency of this pattern by forcing hexagonal boundary conditions. First, only a central part of the grid, of hexagonal shape, has been let open to the flow by putting a hexagonal mask above the grid, whose vertices are touching the previous circular boundary of the grid. In addition, this hexagonal perimeter has been reinforced below the grid, by six vertical thin Teflon walls (thickness 1 mm), replacing the previous vertical circular wall surrounding the whole grid. These thin Teflon walls, and the resulting patterns are visible in Fig. 5a. As it appears in this figure, there are many less defects and it is even possible to create a static pattern. For both viscosities used (20 and 50 cP), it is however still difficult to obtain such a static pattern. To achieve this, one has to correctly tune initial conditions (number and positions of columns) by means of thin needles: after touching the top of a column, one can drive this column to another position by moving the needle, owing to capillary effects. By driving two needles at the same time, it is even possible to gather two columns into one, or to initiate the birth of a column in a place in which the distance between neighbors is too large. A static state appears more easily if the pattern is shrunk, so that it is necessary to provoke the births of several columns. Figure 5a represents a quasi-static networks of columns, and only a careful observation allows the detection of the slow motions of columns around equilibrium positions.

In spite of visibly non-perfectly homogeneous patterns, a clearer hexagonal tendency is demostrated within the entire range of flow-rates. Let us note here that a pattern can be globally static and not homogeneous. These two conditions are incompatible in the 1-D array of columns, where a static pattern is always spatially homogeneous. In 1-D indeed, even the smallest inhomogeneity leads to collective motions of columns, like drifting domains, or a transient slow global drift that restores homogeneity due to phase diffusion (Brunet et al. 2001). However, as in 1-D arrays, one obtains static cells within shrunk patterns, i.e., for the smallest spatial wavelengths. It is of course necessary to provoke the births of lots of columns by the 'needle-method' described above. The distance between static columns is between 1 and 1.2 cm, whereas moving columns generally have a spacing between 1.5 and 2 cm from their nearest neighbors.

We have also tried to build Voronoi diagrams, which offers a different way to visualize the hexagonal tendency of the pattern. An example is reproduced in Fig. 6 for a static pattern, in which each cell is a Voronoi cell

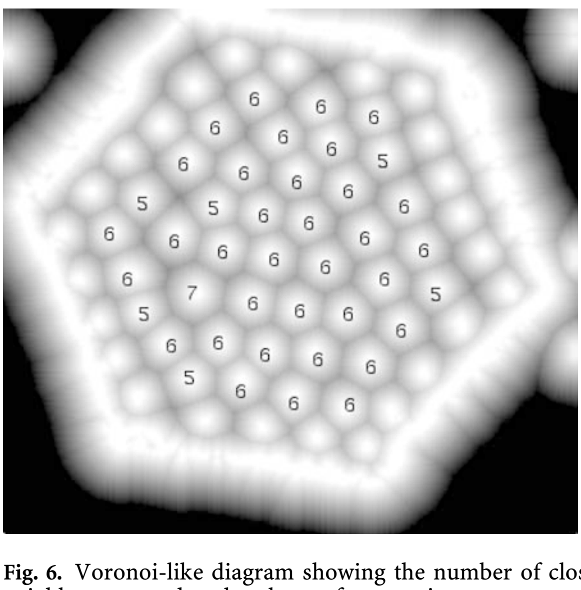

Fig. 6. Voronoi-like diagram showing the number of closest neighbors around each column, for a static pattern

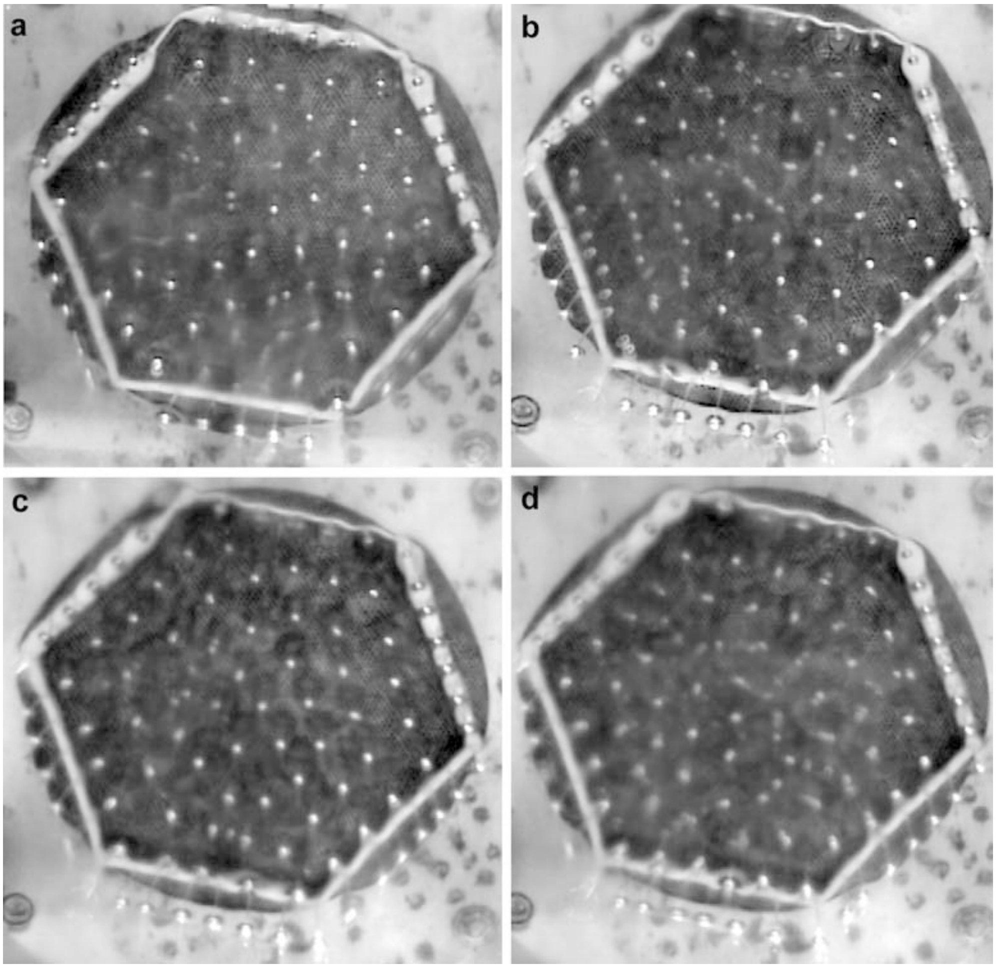

Fig. 7. a–d Temporal averages in turbulent regimes (η=50 cP) with hexagonal boundaries and for different initial conditions (Q=28.2 cm^3/s)

surrounding a column: this is obtained by image-processing which dilates the brightest areas. Into each polygon we have written the number of first neighbors: we can notice that a pattern of columns can stay static even if there exist abnormal cells in regards to the perfect hexagonal network (i.e., with a number of first neighbors different from six).

In most experimental conditions (flow-rate and initial positions of columns), the number of columns fluctuates, in a state comparable to the spatio–temporal chaotic regime observed in the circular dish experiment (Brunet 2002; Brunet et al. 2001). Erratic births of columns or coalescence of two columns into one are observed, and these defects are responsible for the sustenance of unpredictable motions. This means in other words that the dynamics of the pattern will be predictable only if the number of columns keeps constant. The rate of births/coalescences increases with the flow-rate, which is also observed in the one-dimensional similar chaotic pattern.

Contrary to studies of 1-D patterns, one cannot acquire the complete set of column motions by spatio–temporal diagrams. The dynamics of the pattern is accessible only through reduced pictures. We can for example represent pictures of temporal means: these are simply the result of a calculation of temporal mean values of grey levels, by acquiring successive frames. This kind of mean motion-picture has already been used in others systems (Ning et al. 1993). Figure 7 give examples of such means, during long-lasting acquisitions of 1,000 s, from different initial conditions. The rate of acquisition is one frame per second.[1] Columns that remained static during the acquisition appear as the brightest white spots. Displacements of columns appear as smooth white tracks. Clear tracks represent lines along which column motions focused. In all the means reported here, one observes the following remarkable feature: even after long turbulent regimes, there exist small domains of static columns. These static domains coexist with turbulent ones, with sharp separations. Into turbulent domains, one can also observe two close spots, as evidence of oscillations between two limit positions. Generally, erratic births and coalescences of columns are observed in turbulent domains, which sustain chaotic motions. In the 1-D array of columns, a single defect in the spatio–temporal structure leads to a global contamination of disorder (see Fig. 8). Indeed in 1-D, defects launch small drifting domains that propagate in the pattern and are about to collide, creating other defects and sustaining unpredictable spatio–temporal disorder.

[1]This low frequency, chosen to allow long-lasting acquisitions without any memory limitations, does not affect means: temporal means from shorter acquisitions (1 min), but with a higher frequency of 25 frames per second, do not provide any further information.

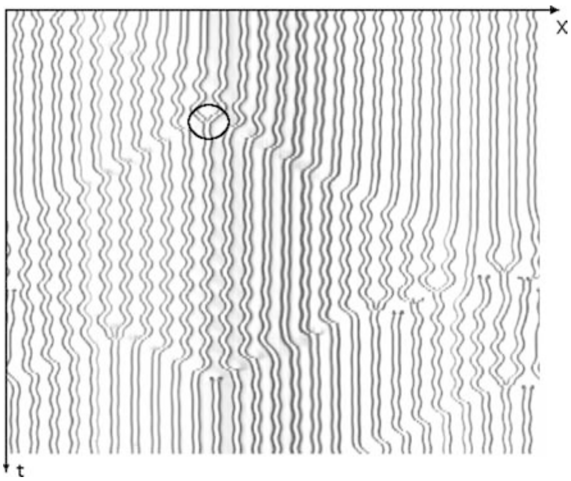

Fig. 8. Spatio–temporal diagram in the 1-D array of liquid columns, providing the motion of each column. A defect (here, inside the circle, the coalescence of two columns into one) sustains disorder by launching two small drifting domains that will encounter and create other defects

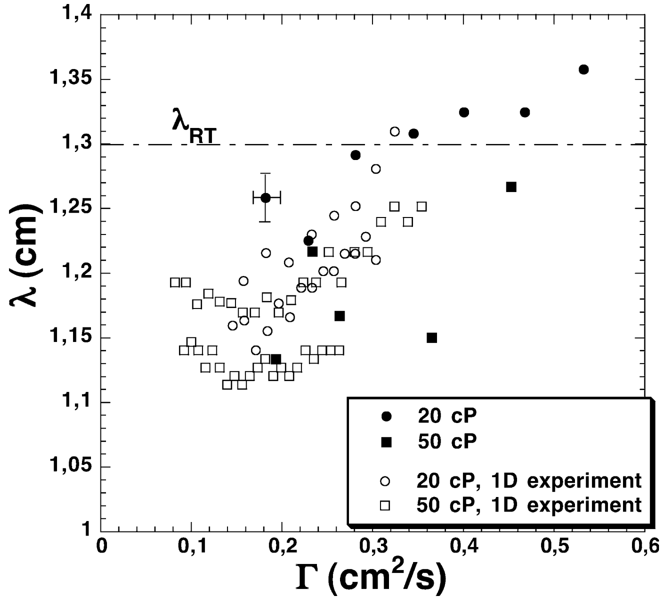

Fig. 10. Mean wavelength between two arrays of columns (*filled symbols*). Reference wavelengths measured on the circular fountain experiment (Counillon et al. 1998; Brunet 2002) are marked by *open symbols*. The most unstable Rayleigh–Taylor wavelength for silicon oils is suggested by the *dashed line*

This contamination process seems to be inhibited in 2-D. Fronts separating static and turbulent domains are stable over a long time, allowing the coexistence of both static and turbulent domains, which is impossible in the 1-D array.

The same kind of temporal means have also been done with circular boundary conditions (Fig. 9a and b). Here, the spatial distribution of disorder is more homogeneous, and turbulent domains extend almost through the whole pattern. Because of boundary conditions which do not fit with the natural hexagonal tendency of the pattern, edges seem to be sources of defects.

4 Some quantitative results

From autocorrelation pictures, one can extract the mean wavelength in both static and turbulent regimes. This wavelength is evaluated at the first maximum of grey levels. These measurements are plotted in Fig. 10, versus flow-rate per unit length Γ, for two viscosities (20 and 50 cP). Γ is defined as the flow-rate per unit surface (the flow-rate divided by the surface of the porous medium) times the mean wavelength. One observes a slight increase with flow-rate, and λ is larger for 20 cP than for 50 cP. With open symbols, we have also plotted measurements from the 1-D circular fountain experiment. Remarkably, the results are very close when one compares the 1-D and 2-D geometry. Let us also note that all these values are close to the most unstable wavelength of the Rayleigh–Taylor instability recalled in Eq. 1, which is equal to nearly 1.3 cm for silicon oils.

In addition to the above qualitative approach of turbulent regimes, it has also been possible to extract measurements during predictable behaviors. Figure 11a illustrates an example of a localized periodic oscillation of a column (this also leads to a weaker-amplitude oscillation of one of its neighbors). A local spatio–temporal diagram of this oscillation can be obtained by extracting grey levels along the line of displacement of the column (Fig. 11b). Values of angular frequency are plotted in Fig. 11c. This frequency grows with the flow-rate, with a law close to $(\Gamma-\Gamma_c)^{1/2}$. These results have qualitative similarities with the ones obtained in 1-D, but Γ_c is here quite large (it is close to zero in 1-D). In 2-D, the angular frequency seems

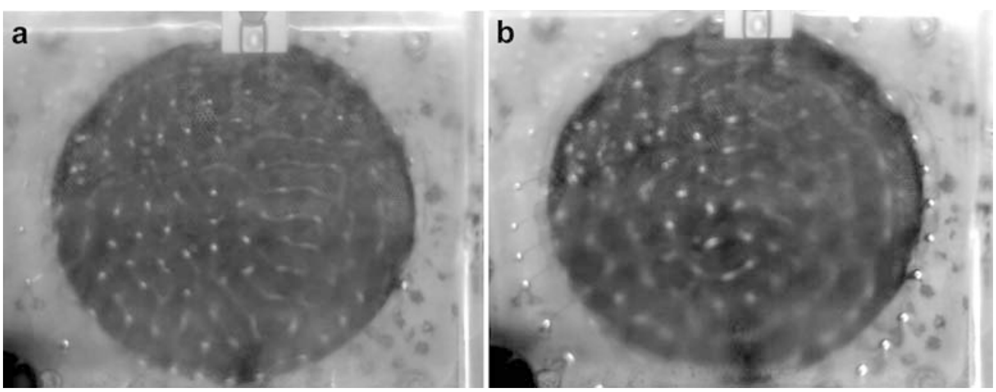

Fig. 9a, b. Temporal averages in turbulent regimes with circular boundaries (η=50 cP). **a** Q=26.0 cm^3/s and **b** Q=64.0 cm^3/s

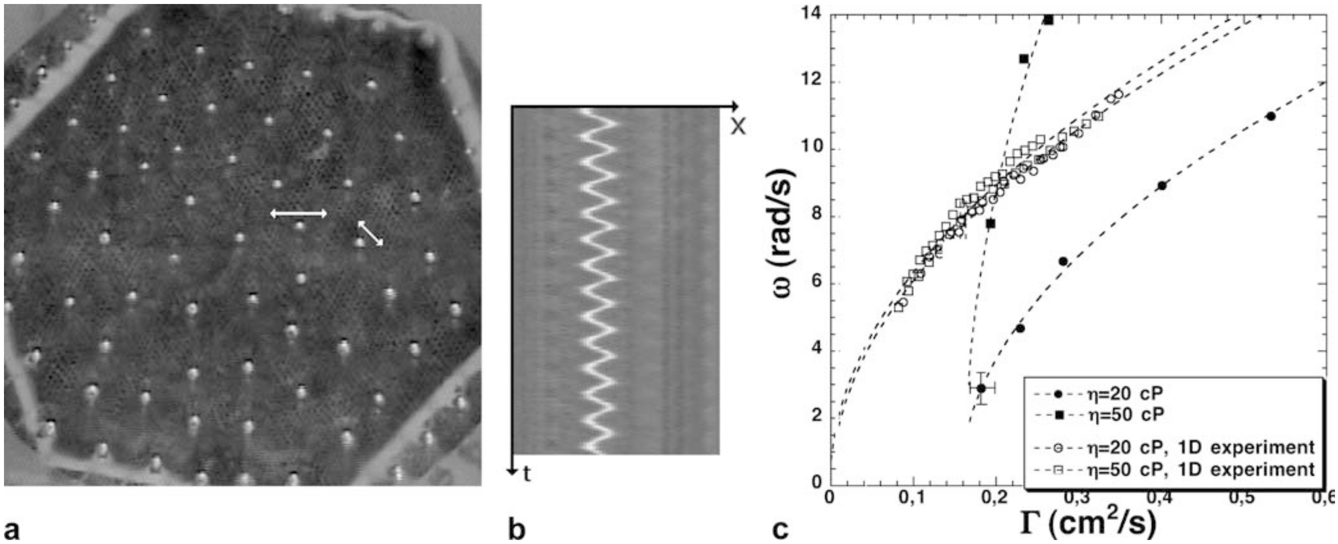

Fig. 11a–c. Measurements of some dynamical quantities (silicon oil 20 and 50 cP). **a** Localized oscillation (η=50 cP, Q=26 cm^3/s). **b** Spatio–temporal diagram of an oscillation. **c** Angular frequency of oscillations (*filled symbols*), *dashed line* representing a fit with $(\Gamma-\Gamma_c)^{1/2}$. Angular frequencies measured on the circular fountain experiment (Counillon et al. 1998; Brunet 2002) are represented by *open symbols*

to increase with viscosity, which is not observed in 1-D. Moreover, the range of flow-rate within oscillations that can appear is more restricted in the 2-D experiment. A possible reason for these discrepancies is that, contrary to the 1-D array of columns where oscillations can extend to the whole pattern, the oscillations here are localized into a very reduced area including at most two or three columns. These oscillations are thus not really the equivalent of the spatial-period doubling regime in interfacial one-dimensional patterns, particularly in the fountain experiment.

5
Discussion, Conclusions

This study enlightens several features of a bidimensional network of liquid columns. Comparisons between the 1-D and 2-D cases show close similarity with what concerns the wavelength selection. In both cases, one gets results very close to the classical Rayleigh–Taylor instability of a thin layer and the same kind of dependence upon flow rate and viscosity.

One also observes similar oscillating motions of columns in 1-D and 2-D. Frequencies seem to grow exponentially with flow-rate, exponents being close to one half, despite differences in thresholds and pre-factors. Another significant difference between 1-D and 2-D concerns the presence of stable fronts separating static and turbulent domains in 2-D. In 1-D, it is not possible to observe such a coexistence: the defects are never localized and due to propagative drifting domains, they tend to spread all along the pattern. In 2-D, such contaminating processes seem to be limited: even if defects sustain disorder, turbulent motions can still be localized in domains which do not spread across initially static ones. The positions of turbulent and static areas depend on initial positions of columns. This is presumably in relation to the fact that we have observed non-homogeneous static patterns and localized oscillations. These differences from 1-D arrays may denote the absence of phase diffusion in our 2-D experiment. In 1-D, this phase diffusion acts as a homogeneity process that slowly tends to restore an equal spacing between columns, and may produce global collective motions of columns. In other words, each column is sensitive to what happens everywhere in the pattern. This behavior does not seem to be so prevalent in 2-D.

Qualitative observations have shown comparable behaviors with a similar experiment developed at the *Institut Non-Lineaire de Nice* (INLN) (Pirat et al. 2004), in which other particular regimes, like the oscillation of a whole array of columns or a 'phase wave' along an array, have been noticed. Contrary to this last experiment, our experiments do not exhibit a perfect hexagonal network, presumably because the geometrical constraints on boundary conditions are less selective.[2] In our system however, a static hexagonal pattern can exist even if the spatial distribution of columns is not homogeneous. In some static cases, the number of first neighbors can locally be different from six. Autocorrelation operations reveal a hexagonal tendency: this is more significant if the pattern is static, but also appears for turbulent patterns.

References

Berenson J (1962) Instability of vapor films during heat transfers. Int J Heat Mass Transf 5:985

Brunet P (2002) Structure et dynamique non-linéaire de liquides tombants. PhD Thesis, Université Pierre et Marie Curie, Paris VI. http://tel.ccsd.cnrs.fr/documents/archives0/00/00/22/42/index_fr.html

Brunet P, Flesselles J-M, Limat L (2001) Parity breaking in a one-dimensional pattern: A quantitative study with controlled wavelength. Europhys Lett 56:221

Carlomagno GM (1974) Moto di un filmo liquido su un cilindro orizzontale posto in aria calma. In: Proceedings of 2nd AIMETA Congress, Naples, p 253

Chandrasekhar S (1961) Hydrodynamic and hydromagnetic stability. Dover, New York

[2] In the INLN's experiment, peripheral columns are forced to a hexagonal network of suspended needles, at an appropriate wavelength.

Counillon C, Daudet L, Podgorski T, Limat L (1998) Dynamics of a liquid column array under periodic boundary conditions. Phys Rev Lett 80:2117
Cross MC, Hohenberg PC (1993) Pattern formation outside of equilibrium. Rev Mod Phys 65:851
Fermigier M, Limat L, Wesfreid JE, Boudinet P, Quilliet C (1992) Two-dimensional patterns in Rayleigh–Taylor instability of a thin layer. J Fluid Mech 236:349
Flesselles JM, Simon AJ, Libchaber AJ (1991) Dynamics of one-dimensional interfaces: An experimentalist's view. Adv Phys 40:1
Ganic EN, Roppo MN (1980) An experimental study of falling liquid film breakdown on a horizontal cylinder during heat transfer. Trans ASME 102:342
Giorgiutti F, Limat L, Weisfreid JE (1995) Dynamics of a one-dimensional array of liquid columns. Phys Rev Lett 74:538
Hu X Jacobi AM (1998) Departure-site spacing for liquid droplets and jets falling between horizontal circular tubes. Exp Therm Fluid Sci 16:322–331
Hynes TP (1978) Stability of thin films. PhD Thesis, Cambridge University
Limat L (1993) Instabilité d'un liquide suspendu sous un surplomb solide: Influence de l'épaisseur de la couche. CR Acad Sci Paris 317:563
Ning L, Ecke RE, Ahlers G (1993) Spatial and temporal averages in chaotic patterns. Phys Rev Lett 71:2216
Pirat C, Mathis C, Maissa P, Gil L (2004) Phys Rev Lett 104:501
Plesset M, Whipple CG (1974) Phys Fluids 17:1
Pritchard GM (1986) Instability and chaotic behaviour in a free-surface flow. J Fluid Mech 165:1
Rayleigh Lord (1900) Scientific papers. Cambridge University Press, Oxford, vol II
Taghavi K, Dhir VK (1980) Taylor instability in boiling, melting, condensation or evaporation. Int J Heat Mass Transf 23:1433
Taylor GI (1950) The instability of liquid surfaces when accelerated in a direction perpendicular to their planes. In: Proc R Soc London A(201):192
Whitehead JA, Luther DS (1975) Dynamics of laboratory diapir and plume models. J Geophys Res 80:705
Yiantsios S, Higgins BG (1989) Phys Fluids A 1:1484